C.P. No. 480
(19,631)
A.R.C. Technical Report

C.P. No. 480
(19,631)
A.R.C. Technical Report

MINISTRY OF AVIATION

AERONAUTICAL RESEARCH COUNCIL

CURRENT PAPERS

The Rotating Flap as a High-Lift Device

by

L. F. Crabtree

LONDON: HER MAJESTY'S STATIONERY OFFICE

1960

FOUR SHILLINGS NET

THE ROTATING FLAP AS A HIGH-LIFT DEVICE

Errata

The following corrections should be made to the text:

Page 8. C_{L_R} is defined as the lift coefficient acting on the complete system but due solely to the rotation of the flap. This is given as the difference between the C_L at a given value of U/V and the C_L with flap fixed ($\beta = 45^o$). However, this value of C_{L_R} still includes the effect of the flap acting as an ordinary flap on the wing through all its angles of rotation.

This effect is eliminated by interpolating for the value of C_L at $U/V = 0$, from Fig. 9. At low angles of incidence, the lift coefficient at $U/V = 0$ is close to that for a fixed flap angle, $\beta = 45^o$.

Now equation (4) of Appendix I gives

$$\frac{\Gamma + \Gamma_o}{2\pi a V} = 2 \sin \alpha + \frac{\lambda - \frac{1}{\lambda}}{\lambda + \frac{1}{\lambda} - 2 \cos \varphi} \cdot \frac{\Gamma}{2\pi a V} .$$

In Fig. 5, the circulation around the wing = Γ_o

$$\therefore \quad C_{L_{wing}} = \frac{\Gamma_o}{2 a V}$$

$$\therefore \quad C_{L_R} = \frac{\Gamma_o}{2 a V} + \frac{\Gamma}{2 a V} - 2\pi \sin \alpha$$

$\therefore$ From equation (4)

$$C_{L_R} = \left(\frac{\lambda - \frac{1}{\lambda}}{\lambda + \frac{1}{\lambda} - 2 \cos \varphi} \right) \cdot \frac{\Gamma}{2 a V}$$

$$\therefore \quad C_{L_R} - C_{L_f} = \frac{\Gamma}{2 a V} \{ f(\lambda, \varphi) - 1 \} .$$

Page 9. The value given for $f(\lambda, \varphi)$ in position 2 is incorrect.

By iteration of the transformation equations in Appendix I, for $\frac{x}{a} = 2.20$, $\frac{y}{a} = -0.52$ we obtain $\lambda = 1.855$ and $\cos \varphi = 0.9186$.

Hence $f(\lambda, \varphi) = 2.363$.

The effects of these corrections on the table on page 9 are as follows:

U/V	$R = \frac{V \cdot c}{\nu}$	V m/s	α^o	C_{L_R}	Γ	Γ_{theor}	Γ/Γ_{theor} %
			5	2.11	0.64		20.3
4.0	0.14×10^6	6.8	10	2.075	0.63	4.47	20.1
			15	2.075	0.63		20.1
			5	1.025	0.71		19.6
2.0	0.32×10^6	15.5	10	1.00	0.69	5.16	19.1
			15	1.00	0.69		19.1

These values of Γ/Γ_{theor} compare very closely with the values (for low values of U/V) on an isolated flap as given in the Table on Page 8.

The above calculations are due to Mr. A.P. Cox.

C.P. No. 480

U.D.C. No. 533.691.152.4

Technical Note No. Aero 2492

April, 1957

ROYAL AIRCRAFT ESTABLISHMENT

The rotating flap as a high-lift device

by

L. F. Crabtree

With an Appendix by D. A. Kirby

SUMMARY

It is well-known that a wing in an airstream can develop extremely high values of lift coefficient if it is rotated about a spanwise axis. A more practical development of this system is a fixed mainplane with a rotating trailing-edge flap. The results of some little-known German research on both systems have been collected together and are presented in compact form together with some further analysis. The emphasis is on the wing-rotating flap combination, and it is shown that this is a very attractive way of generating high lift. Some gaps in our knowledge of the device are pointed out and suggestions are made for some further research.

LIST OF CONTENTS

LIST OF APPENDICES

LIST OF ILLUSTRATIONS

LIST OF SYMBOLS

A — Wing aspect ratio

a = $c/4$ (see Fig.5)

c — Wing chord

c_f — Flap chord

C_D — Drag coefficient

C_L — Lift coefficient

C_{L_f} — Coefficient of lift on flap (see Section 5)

C_{L_R} — Increment in lift coefficient due to rotation of flap (see Section 5)

$C_{m\ c/4}$ — Pitching moment about quarter-chord point

C_R — Power coefficient = $\dfrac{M}{\frac{1}{4}\rho U^2 Sc}$

E — Efficiency of rotating flap: $E = \dfrac{\Gamma}{\Gamma_{theor}}$ (see Section 5)

H — Endplate height

L — Total (measured) lift

M — Turning moment applied to rotate wing (or flap)

N — Work done per second to rotate wing (or flap)

P — Power required to rotate flap

S — Wing area

S_f — Flap area

t/c — Wing (or flap) thickness-chord ratio

U — Peripheral velocity of wing or flap: $U = \frac{1}{2}\, c.\omega$

V — Velocity of main stream

V_A — Approach speed of aircraft

V_S — Stalling speed of aircraft

$w = v_x - i\, v_y$. Complex velocity in ζ-plane

$z = x + iy$. Co-ordinates in physical plane (Fig.5)

α — Incidence of wing

β — Flap angle

κ — "Endplate effect" correction to aspect ratio

λ — Measure of distance between wing and rotating flap: see Fig.5.

ω — Angular velocity of rotating wing (or flap)

$\zeta = \xi + i\eta$. Co-ordinates in transformed plane (see Fig.5).

---

1 Introduction

From time to time numerous devices have been proposed for producing high lift forces on aircraft wings, and considerable effort is currently being expended on some of these schemes. One particular device to which less attention has been devoted than appears to be merited is the rotating flap, or auxiliary wing, mounted just below the trailing-edge of the main-plane. Some research was carried out on this scheme a long time ago and again in Germany during the 1939-1945 period, and the purpose of this report is to collect together the results obtained in that work, and to present them together with some further analysis. Thus it is hoped to emphasize the potential value of the rotating flap as a high-lift device.

Some experimental results for an isolated rotating wing are presented first, and the phenomena of autorotation and of the Magnus effect are discussed. The thin aerofoil theory of a wing with a rotating trailing-edge flap is developed, and experimental results for such a configuration are given. The final discussion includes a correlation between the results for the wing with rotating flap and for an isolated rotating wing.

2 Experimental results for a rotating wing

In the case of an isolated rotating wing, two separate phenomena are involved. It has been known for some time that a lifting surface such as a wing in a mainstream can develop high lift by rotation about a spanwise axis, and at high rotational speeds the phenomena is similar to the Magnus effect on a circular cylinder. At lower rotational speeds however the phenomenon of autorotation is displayed. The latter was studied by Maxwell[1] in the case of an inclined plane lamina allowed to fall freely. Mouillard[2] has also studied this problem. Measurements of the frequency of autorotation as a function of mainstream velocity and wing chord were made by Joukowsky[3] and the results have been presented by von Holst[4] together with the results of his own experiments. It was surmised that in general the ratio of peripheral velocity, U, in auto-rotation, to mainstream velocity, V, was constant at about 0.5. Later experiments by Küchemann showed that in fact the thickness-chord ratio, t/c, has a definite effect as shown in Fig.1.* It appears beneficial to use thinner sections, for which higher speeds of autorotation are obtained, and of course the drag of such sections would be expected to be smaller.

Higher lift can be obtained by rotating the wing at speeds greater than that of autorotation. Curves of the lift coefficient of various configurations as a function of U/V are replotted from reference 5 in Fig.2, and the corresponding drag polars are given in Fig.3. It will be seen that end plates have a significant effect in increasing the lift and (at all but the highest lift coefficients) decreasing the drag. The maximum values of lift coefficient reported in reference 5 were about 8 to 12, the corresponding values of U/V being between 8 and 10. Thus higher values of the ratio $C_{L\,max}$ (with rotation) to $C_{D\,min}$ (without rotation, in high speed flight) can be obtained than with most other systems.

The question of the power absorbed in rotating a wing at speeds above that characteristic of autorotation has been investigated by H Wiese[6]. A power coefficient is defined as

$$C_R = \frac{M}{\frac{1}{2}\rho U^2 . S . \frac{c}{2}} = \frac{N}{\frac{1}{2}\rho U^3 . S}$$

---

* That these curves do not pass through the origin is simply a consequence of the friction in the bearings.

where $U = \frac{c}{2} \cdot \omega$ is the peripheral velocity of the wing rotating about the centre of the chord, c, the surface area being S. M is the turning moment applied to the wing, and N the work done per sec in rotating the wing.

Some of the results obtained by Wiese are presented in Fig.4 in which the power coefficient C_R is plotted against the ratio U/V for the wing of reference 5, (symmetrical biconvex circular-arc section, $t/c = 0.167$, and aspect ratio 2). Tests were made both with and without endplates.

In the range of U/V values for which maximum lift coefficients are attained, the coefficient of power required for rotation is not substantially different from that required in stationary air ($U/V = \infty$). These results are rather incomplete; but assuming them to hold also for a wing with rotating flap, a simple calculation has been made in Appendix II to estimate the power required for reducing the approach speed of a typical four-engined subsonic transport aircraft.

3 Theory of a wing with rotating flap

In view of the practical difficulties associated with the isolated rotating wing, an obvious development was a wing with a rotating flap situated just below the trailing-edge. This can ideally be represented by a flat plate together with a vortex at the axis of rotation of the flap. Thin aerofoil theory can be developed for this ideal case and it can be solved by the potential flow method of conformal transformation. This is closely related to the case of the two-dimensional jet-flapped aerofoil, where the jet can be represented by a continuous distribution of vorticity in contrast with the concentrated vortex of the present theory.

The appropriate transformation is

$$z = \zeta + \frac{a^2}{\zeta}$$

whereby a circle of radius a in the ζ-plane is transformed into a slit of length $c = 4a$ along the real axis of the z-plane. The two planes are shown in Fig.5. The details of the calculation are given in Appendix I where it is shown that, using the Kutta condition at the trailing-edge, the lift on the mainplane per unit span is

$$C_L = 2\pi \cdot \sin \alpha + 2f(\lambda,\varphi) \cdot \frac{\Gamma}{Uc}$$

where Γ is the strength of the vortex representing the rotating flap and $(a\lambda,\varphi)$ are the polar co-ordinates of its position in the circle - or ζ-plane. The relation between the physical parameters of the rotating flap (e.g. U/V) and the vortex strength, Γ, is not yet known. The adequacy of the Kutta-Joukowsky condition is also questionable, and further experiments are needed to investigate both of these points.

The position of the vortex which gives the maximum lift for a given incidence of the mainplane can be calculated by differentiating $f(\lambda,\varphi) = F(\xi,\eta)$ w.r.t. ξ say, holding η (the ordinate in the ζ-plane) constant. The condition is shown in the appendix to be $\xi = a - \eta$, and this result has been transformed back into the physical - or z-plane to yield the curve shown in Fig.6.

It may also be noted that the condition $\xi = a + \eta$ yields a minimum under the same assumptions.

4 Experimental results for a wing with rotating flap

The experiments reported by von Holst[4] have been extended by Küchemann[7] who tested a rectangular wing-flap combination fitted with elliptical endplates. Both wing and flap were of NACA 23015 section; the mainplane had a chord c = 30 cm and a span of 80 cm. The flap chord was 0.25 c and it was pivoted at its midpoint. Three different positions of the rotating flap relative to the mainplane were tested, the co-ordinates of the axis of rotation referred to the mainplane trailing-edge as origin were as follows:-

Position	x/c	y/c
1	-0.13	+0.18
2	+0.05	+0.13
3	+0.13	+0.10

These are shown in Fig.8. Of these positions the second was theoretically the best (as described in Section 3, and indicated in Fig.6) whilst the first roughly corresponds to a position of minimum efficiency.

The peripheral speed, U, of the flap in autorotation is roughly constant for a given position of the flap and a given mainstream velocity, V, over a fairly wide range of incidence. The variation of the ratio U/V in autorotation with flap position is shown in Fig.7, and it may be remarked that below a speed of about 10 m/s, the mainstream has insufficient energy to promote autorotation of the flap.

The values of maximum lift coefficient $C_{L\ max}$ with the three different flap positions are plotted against the ratio U/V in Fig.8. It is seen that the theoretical prediction of position 2 as the most efficient in producing lift was confirmed. The sudden drop in $C_{L\ max}$ with the flap in this position for $U/V > 4$ is due to a laminar separation on the mainplane, the test Reynolds number of 0.14×10^6 being too low to ensure transition to turbulence in the boundary layer well forward on the wing. The separation first occurred in the endplate junctions and was present to a certain extent throughout the whole test range. At the much higher full-scale Reynolds numbers and in the absence of endplates the boundary layer would be turbulent and this reduction in $C_{L\ max}$ would either not occur, or be postponed to a higher value of U/V. This is simply because a turbulent boundary layer is better able to withstand the larger, adverse pressure gradients associated with higher values of U/V without separating. For any future tests a transition wire would of course be fitted in order to eliminate this scale effect.

Detailed lift curves with the flap in position 2 are shown in Fig.9 for a range of U/V values. These may be compared with results for the fixed flap on the same figure. As previously stated, the loss of lift as U/V is increased above 4 is caused by a laminar separation due to the low Reynolds number of the tests.

Corresponding drag polars are plotted in Fig.10. Also included are curves for negative values of U/V, and these demonstrate the effectiveness of such a configuration as an airbrake. This is emphasized in the lift, drag and pitching moment curves of Fig.11 for all three flap positions

at $U/V = -2$. For instance with the flap in position 2 at zero lift (actually a small positive incidence), C_D is comparatively large but there is only a small (nose-down) pitching moment.

Large trim changes are to be expected when the rotating flap is in operation and producing high lift. The pitching moment coefficient, $C_{m\ c/4}$, at maximum lift is plotted against U/V in Fig.12, for the three flap positions. Detailed curves of $C_{m\ c/4}$ against C_L are plotted in Fig.13 for flap position No.2 for various values of U/V. Curves for the flap fixed configuration are again shown for comparison.

5 Efficiency of the rotating flap

The efficiency of the means by which a rotating flap produces high lift may be gauged from an analysis of the results of Ref.7. A similar analysis may be carried out for the isolated rotating wing of Ref.5, and the two systems may be compared. Such a comparison is based on the circulation produced about its own axis by the rotating wing or flap; an extremely simple theoretical estimate of this circulation may be considered:-

$$\Gamma_{theor} = U \pi c_f$$

so that

$$C_L = 2\pi \cdot \frac{U}{V}$$

where U is the circumferential velocity of the flap or rotating isolated wing and c_f is the chord length of the flap. For wings of finite aspect ratio the factor 2π may be replaced by

$$\frac{2\pi}{1 + \kappa \cdot \frac{2}{A}}$$

where κ is the usual correction factor depending on the ratio between endplate height and the wing span. The actual circulation generated, Γ, is obtained from the Kutta formula for lift

$$L = \rho V \Gamma$$

where L is the measured lift and V the mainstream velocity.

For the isolated rotating wing therefore

$$\Gamma = \tfrac{1}{2} C_L V c_f .$$

Analysis of the results of reference 5 for an aspect ratio 5 wing of 0.12 m chord, 0.167 t/c, biconvex circular arc section, fitted with end-plates, gave the following table:-

C_L	U/V	V m/s	U m/s	Γ m^2/s	Γ_{theor} m^2/s	Γ/Γ_{theor} %
12.6	10	4.1	41	3.10	12.8	24.2
10.45	8	5.1	41	3.20	12.8	24.9
8.0	6.85	6.0	41	2.90	12.8	22.6
6.55	5.85	7.0	41	2.75	12.8	21.4
5.7	5.10	8.0	41	2.75	12.8	21.4
4.45	4.10	10.0	41	2.67	12.8	20.8

For the circular cylinder of A = 12 fitted with endplates, the "efficiency"

$$E = \frac{\Gamma}{\Gamma_{theor}} = \frac{C_L}{2\pi \cdot \left(U/V\right)},$$

or

$$E = \frac{C_L}{2\pi \cdot \left(U/V\right)} \cdot \left(1 + \kappa \cdot \frac{2}{A}\right)$$

for finite aspect ratio, varied from about 30% to 47%. It seems therefore that a thicker section may be more efficient in producing lift as an isolated rotating wing, although it is not certain how much of the increased efficiency of the circular cylinder is due to its higher aspect ratio. From Fig.2 it appears that the efficiency is higher at speeds up to autorotation (U/V approx.0.5).

For the wing with a rotating trailing-edge flap the analysis is a little more complicated. The results plotted in Fig.9 for flap position No.2 have been used, and the method of analysis is as follows:-

The contribution of the lift acting on the flap itself is found from

$$C_{L_f} \times \tfrac{1}{2}\rho V^2 c = \rho V \Gamma$$

$$\therefore C_{L_f} = \frac{2\Gamma}{Vc}$$

where c is the mainplane chord and Γ is the circulation produced by the flap about its axis of rotation.

The lift coefficient acting on the complete system C_{L_R} but due solely to the rotation of the flap is obtained from Fig.9 by subtracting the C_L with fixed flap at a given incidence from the C_L at a given value of U/V. Then we have from equation (4) of the appendix

$$C_{L_R} - C_{L_f} = \frac{2\Gamma}{Vc} \cdot f(\lambda,\varphi)$$

hence $$C_{L_R} = \frac{2\Gamma}{Vc}\,[1 + f(\lambda,\varphi)].$$

Now for flap position No.2, $f(\lambda,\varphi) = 0.272$,

$$\therefore\ \Gamma = C_{L_R} \cdot V \cdot c/2.544 .$$

The theoretical circulation Γ_{theor} produced by the flap about its axis of rotation is again estimated as

$$\Gamma_{theor} = U \pi c_f .$$

An appropriate correction may be made for the effect of finite aspect ratio similar to that proposed above.

Results of the analysis are given in the following table, with $c = 0.3$ m and $c_f = 0.075$ m.

U/V	$R = \frac{V \cdot c}{\nu}$	V m/s	α^o	C_{L_R}	Γ	Γ_{theor}	Γ/Γ_{theor} %
			5	2.61	2.10		47.1
4.0	0.14×10^6	6.8	10	2.50	2.00	4.47	44.7
			15	2.36	1.89		42.4
			5	1.53	2.76		54.2
2.0	0.32×10^6	15.5	10	1.40	2.55	5.16	50.2
			15	1.26	2.30		45.2

The "efficiency" is seen to be greater when the rotating flap operates in conjunction with a fixed mainplane rather than as an isolated rotating wing. This is presumably because the constraint afforded by the trailing-edge of the mainplane and its wake serves to concentrate the circulatory motion produced by the rotating flap.

In any case the "efficiency" of a rotating flap, as defined above, is a very useful criterion and may be used as a basis for comparison in any future tests. It is clear that such tests should include considerations of the effect of flap thickness-chord ratio, the effect of aspect ratio of the wing-flap system, effect of increasing the Reynolds number, and finally an application of the system to a particular aircraft.

6 Conclusions

The results of the test which have been described and analysed show that the combination of a wing and a rotating flap just behind its trailing-edge is a very attractive scheme for generating high lift. This system is a development of work on an isolated rotating wing directed toward the same

end. The latter scheme would however involve severe difficulties in any practical application to an aircraft.

Quite high values of lift can be obtained by simply allowing the flap to autorotate, but a much higher lift is attained by rotating the flap with higher frequencies. The values of the lift increment that can then be achieved are of similar order to those obtained with the jet flap. Some information on the power required to rotate the flap in this latter case is presented, but much more experimental information is required. Applying the data available for the isolated rotating wing as it stands to the case of a wing with rotating flap and using it to calculate the power required in a practical case shows that rather large amounts of power would be required if the approach speed of the aircraft is to be appreciably reduced. However, the information is so limited, and the Reynolds number of the test so low, that much more experimental work is required before this particular application can be seriously considered. If the flap is rotated in the opposite direction (negative values of U/V) it is shown that a very efficient air-brake system results with a possibility of controlling changes of trim.

Further tests would be desirable to check some outstanding questions, and theses should include investigations into

(1) the effect of flap thickness chord ratio and ratio of flap to wing chords,

(2) the actual induced loading on the mainplane, and a check on the adequacy of applying the Kutta condition at the trailing edge,

(3) the effect of aspect ratio and of sweep,

(4) the effect of Reynolds number (the tests reported here were done at quite small values of R).

REFERENCES

No.	Author	Title etc.
1	J.C. Maxwell	Cambridge and Dublin Mathematical Journal, vol.IX, 1853.
2	M. Mouillard	L'empire de l'air, 1881.
3	N. Joukowski	De la chute dans l'air de corps legers de forme allongée, animés d'un mouvement rotatoire. Bulletin de l'Inst.Aerodyn. de Koutchino, 1906.
4	E. von Holst	Der rotierende Flügel als Mittel zur Hochauftriebserzeugung. Jahrbuch 1941 der deutschen Luftfahrtforschung Page I 372.
5	D. Küchemann	Auftrieb und Widerstand eines rotierenden Flügels. Deutsche Luftfahrtforschung, Forschungsbericht No.1651 (A.V.A., Göttingen), 1942.

REFERENCES (Contd.)

No.	Author	Title etc.
6	H. Wiese	Drehleistungsmessungen an rotierenden Flügeln. A.V.A. Göttingen, Report 42/A/14. 1942.
7	D. Küchemann	Drei-komponentenmessungen an einem Flügel mit rotierendem Hilfsflügel. Deutsche Luftfahrtforschung, Forschungsbericht No.1513 (A.V.A. Göttingen), 1941.

APPENDIX I

Theory of an aerofoil with rotating flap

Referring to Fig.5, the z-plane represents the flow about a two-dimensional flat plate with a vortex located below and behind the trailing-edge.

This flow is transformed into a ζ-plane by the conformal transformation

$$z = \zeta + \frac{a^2}{\zeta} \qquad (1)$$

whereby the slit along the x-axis from -2a to +2a in the z-plane becomes a circle of radius a centred on the origin in the ζ-plane.

The complex potential of the flow in the ζ-plane is

$$F(\zeta) = V\left(\zeta . e^{-i\alpha} + \frac{a^2}{\zeta} . e^{i\alpha}\right) + \frac{i(\Gamma + \Gamma_o)}{2\pi} . \ell n\, \zeta e^{-i\alpha} + \frac{i\Gamma}{2\pi} . \ell n \left(\frac{\zeta - \zeta_1}{\zeta - \zeta_2}\right) \qquad (2)$$

where $\zeta_1 = \lambda a\, e^{i\varphi}$ is the position of the vortex of strength Γ which represents the rotating flap in the circle-plane and

$$\zeta_2 = \frac{a}{\lambda} e^{i\varphi}$$

is the position of an equal but opposite vortex at the image point. This image vortex is necessary to make the circle into a streamline of the flow in the ζ-plane. The circulation about the origin is then $(\Gamma + \Gamma_o)$.

The complex velocity is $w = \frac{dF}{d\zeta}$

$$\therefore w = v_x - i . v_y$$

$$= V\left(e^{-i\alpha} - \frac{a^2}{\zeta^2} . e^{i\alpha}\right) + \frac{i(\Gamma + \Gamma_o)}{2\pi} . \frac{1}{\zeta} + \frac{i\Gamma}{2\pi} . \frac{1}{\zeta - \zeta_1} - \frac{i\Gamma}{2\pi} . \frac{1}{\zeta - \zeta_2} . \qquad (3)$$

Putting $w = o$ we obtain an expression for the positions of the stagnation points. Fixing the near stagnation point on the mainplane at the trailing-edge, according to the Kutta-Joukowski condition, enables the circulation about the origin to be determined:-

i.e. put $w = o$ in equation (3) and substitute $\zeta = a$,

$$\therefore \frac{\Gamma + \Gamma_o}{2\pi a V} = 2 \sin\alpha + \frac{\lambda - \frac{1}{\lambda}}{\lambda + \frac{1}{\lambda} - 2\cos\varphi} . \frac{\Gamma}{2\pi a V} . \qquad (4)$$

This reduces to the familiar result of thin aerofoil theory when $\Gamma = o$,

$$\frac{\Gamma_o}{2\pi a V} = 2 \sin\alpha \qquad (5)$$

or, since $$L = C_L \cdot \tfrac{1}{2}\rho V^2 c = \rho V \Gamma_o$$

where $c = 4a$

$$\therefore C_L = 2\pi \cdot \sin \alpha .$$

From equation (4) we see that the lift acting on the system at a fixed incidence and free-stream velocity, for a given value of Γ, is proportional to

$$\frac{\lambda - \frac{1}{\lambda}}{\lambda + \frac{1}{\lambda} - 2\cos\varphi} = \frac{\xi^2 + \eta^2 - a^2}{\xi^2 + \eta^2 - 2a\xi + a^2}, \qquad (6)$$

if we write $\lambda a = \xi + i \cdot \eta$ for the position of the subsidiary vortex Γ in the circle plane.

Holding η constant and differentiating equation (6) w.r.t. ξ we obtain

$$\xi = a \pm \eta$$

for a stationary value of the lift.

Investigation of the second derivative shows that minimum lift occurs under the specified conditions when

$$\xi = a + \eta \qquad (7)$$

and that maximum lift is obtained when

$$\xi = a - \eta . \qquad (8)$$

Relations between the co-ordinates in the z-plane and the ζ-plane are obtained from the transformation (1):-

$$x = \left(1 + \frac{1}{\lambda^2}\right) \cdot \xi$$

$$y = \left(1 - \frac{1}{\lambda^2}\right) \cdot \eta$$

where $$\left(\frac{\xi}{a}\right)^2 + \left(\frac{\eta}{a}\right)^2 = \lambda^2$$

We may therefore construct the locus of best positions of the rotating flap in the physical or z-plane, using equation (8), as in the following table.

η/a	ξ/a	λ^2	$\frac{x}{2a}$	$y/2a$
0	1.0	1.0	1.0	0
-0.5	1.5	2.5	1.05	-0.15
-0.75	1.75	3.625	1.117	-0.27
-1.0	2.0	5.0	1.20	-0.40
-1.5	2.5	9.0	1.39	-0.67
-2.0	3.0	13.0	1.615	-0.92

This locus, represented by the last two columns, is plotted in Fig.6.

APPENDIX II

by D.A. Kirby

Power required to rotate the flap of a typical four-engined transport

The scheme of using a rotating flap works on a principle similar to that of the jet flap and it may therefore be expected that the power required to achieve a given reduction of the approach speed will be of a similar order in both schemes. In the absence of measured values for the rotating flap, an attempt is made here to obtain at least a rough estimate of the power required by using the values measured on an isolated rotating aerofoil, i.e. it is assumed that the powers measured by Wiese (Fig.4) are sufficiently representative of the practical case. It is further assumed that the values of the lift plotted in Fig.9 give a measure of the gains in lift which can be expected. This implies that, without supplying extra power, the autorotating flap gives about twice the lift increment of the slotted flap without rotation. In view of the nature of the available data, it may be expected that the analysis is pessimistic.

The following data obtained from an analysis of several current aircraft have been used in the calculations:-

(i) Flap area S_f = 0.17 × Wing area (S).

(ii) Flap chord c_f = 0.25 × Wing chord (c).

(iii) Flap aspect ratio per side = 7.

(iv) Total available engine horse power = 8 × Wing area in sq ft.

(v) Approach speed (V_A) with flaps down but not rotating = 120 knots, the approach C_L then being 1.2.

(vi) Stalling speed $V_S = V_A/1.3$.

The experimental results of Fig.9 are for a flap chord/wing chord ratio of 0.25. It is considered that this is large for the case of a rotating flap. The same effect on lift coefficient could be obtained with a smaller flap, as it depends primarily on the ratio U/V, in which case the power required could be less than that obtained here.

The power required to drive the flaps is given by:-

$$P = C_R \times \tfrac{1}{2}\rho U^3 S_f$$

or

$$\frac{P}{S} = C_R \times \frac{S_f}{S}\left(\frac{U}{V_A}\right)^3 \tfrac{1}{2}\rho V_A^3$$

where C_R = power coefficient

U = peripheral velocity of flap.

For a flap aspect ratio of 7, C_R has been taken from Fig.4 as 0.15.

Then $\frac{\text{Horse Power}}{S} = 0.15 \times 0.17 \left(\frac{U}{V_A}\right)^3 \times \frac{1189}{550} \left(\frac{V_A}{100}\right)^3$

where V_A and U are in ft/sec

ρ at sea level I.S.A.

$$\frac{H.P.}{S} = 0.055 \left(\frac{U}{V_A}\right)^3 \left(\frac{V_A}{100}\right)$$

$$= 0.121 \left(\frac{U}{V_A}\right)^3 \left(\frac{V_S}{100}\right)^3$$

when $V_A = 1.3\ V_S$.

If it is assumed that the increments in $C_{L\ max}$ when the flap is rotated are 80% of those given in Fig.9 for a full span flap with endplates then V_S and V_A are:-

Flap condition	$C_{L\ max}$	C_L approach	V_S knots	V_A knots	V_A ft/sec
Fixed at $\beta = 45^\circ$	2.03	1.20	92.3	120.0	202.7
Autorotating	2.27	1.34	87.3	113.5	191.7
Driven at $\frac{U}{V_A} = 2$	2.55	1.51	82.3	107.0	180.7
Driven at $\frac{U}{V_A} = 4$	3.38	2.00	71.5	93.0	157.0

and the powers are:-

Flap condition	% reduction in V_A	$\frac{\text{Horse Power}}{S}$ for $C_R = 0.15$
Autorotating	5.4	0
Driven at $\frac{U}{V_A} = 2$	10.9	2.6
Driven at $\frac{U}{V_A} = 4$	22.5	13.6

Thus reductions in the approach speed of up to 7 or 8% could be achieved with a small power. Further reductions would become very costly and the use of all four engines to drive the flap would only reduce the approach speed by 17%.

It is unlikely that much power could be diverted to drive the flap because of

(i) the performance requirements with one engine cut and for a baulked landing,

(ii) the reduction in lift/drag ratio when the flap is rotated (Fig.10). This is largest when the flap is autorotating.

The data used above were all obtained from tests at a low Reynolds number. The higher $C_{L\ max}$ which will be obtained full scale at the same U/V will allow further reductions in the approach speed and a decrease in the power required. The above analysis emphasises the importance of obtaining more extensive and reliable data before a proper assessment of the scheme can be made. Further, it will be essential to reduce the size of the rotating flap in comparison with that of a conventional flap to make best use of the scheme.

WT.2078.C.P.480.K3 - Printed in England

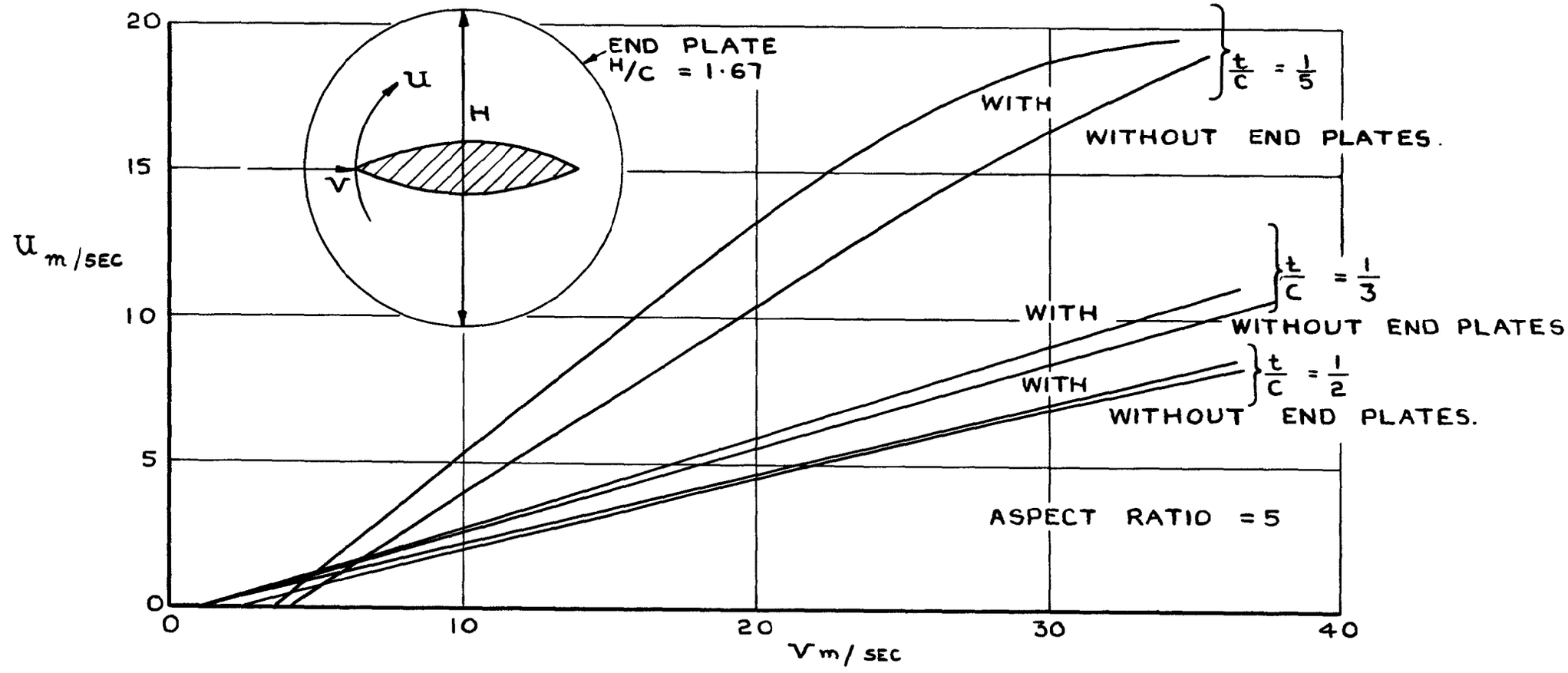

FIG. 1. AUTOROTATION OF BICONVEX CIRCULAR-ARC SECTIONS.

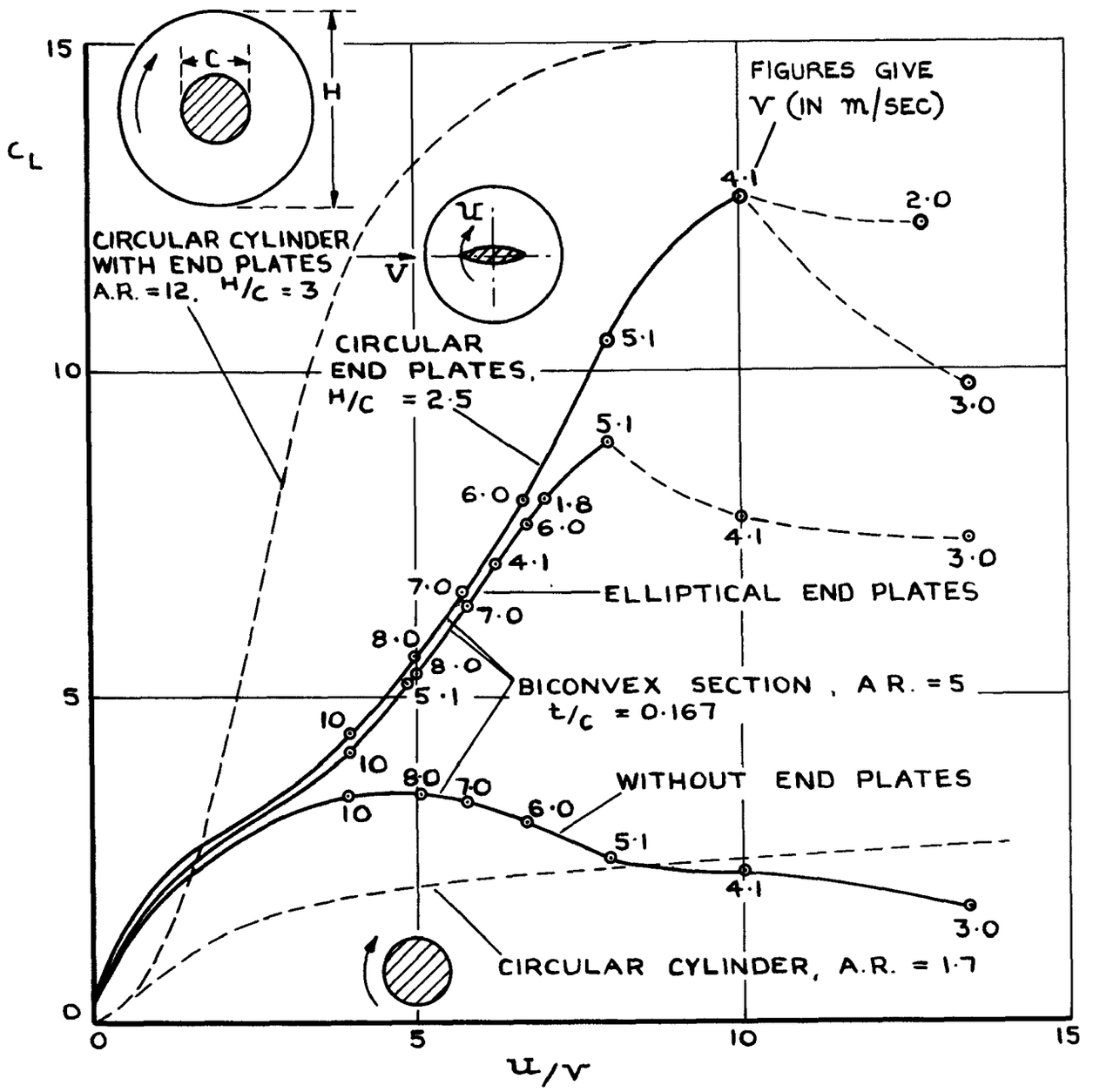

FIG. 2. LIFT COEFFICIENT AS A FUNCTION OF THE RATIO OF PERIPHERAL AND FREE-STREAM VELOCITIES FOR ROTATING CIRCULAR CYLINDER AND BICONVEX CIRCULAR-ARC SECTION WITH AND WITHOUT END PLATES.

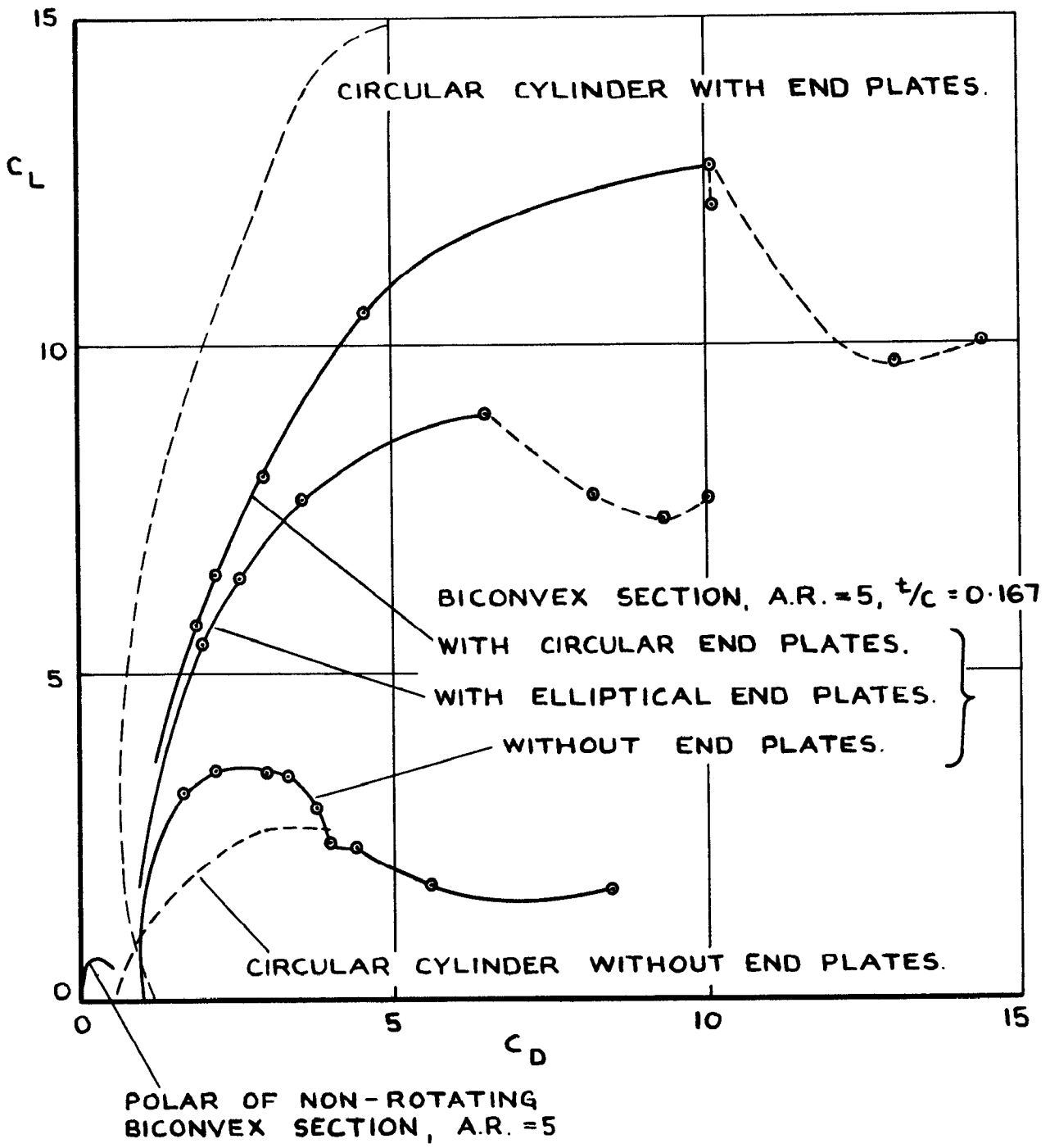

FIG. 3. DRAG POLARS FOR THE CONFIGURATIONS OF FIG. 2.

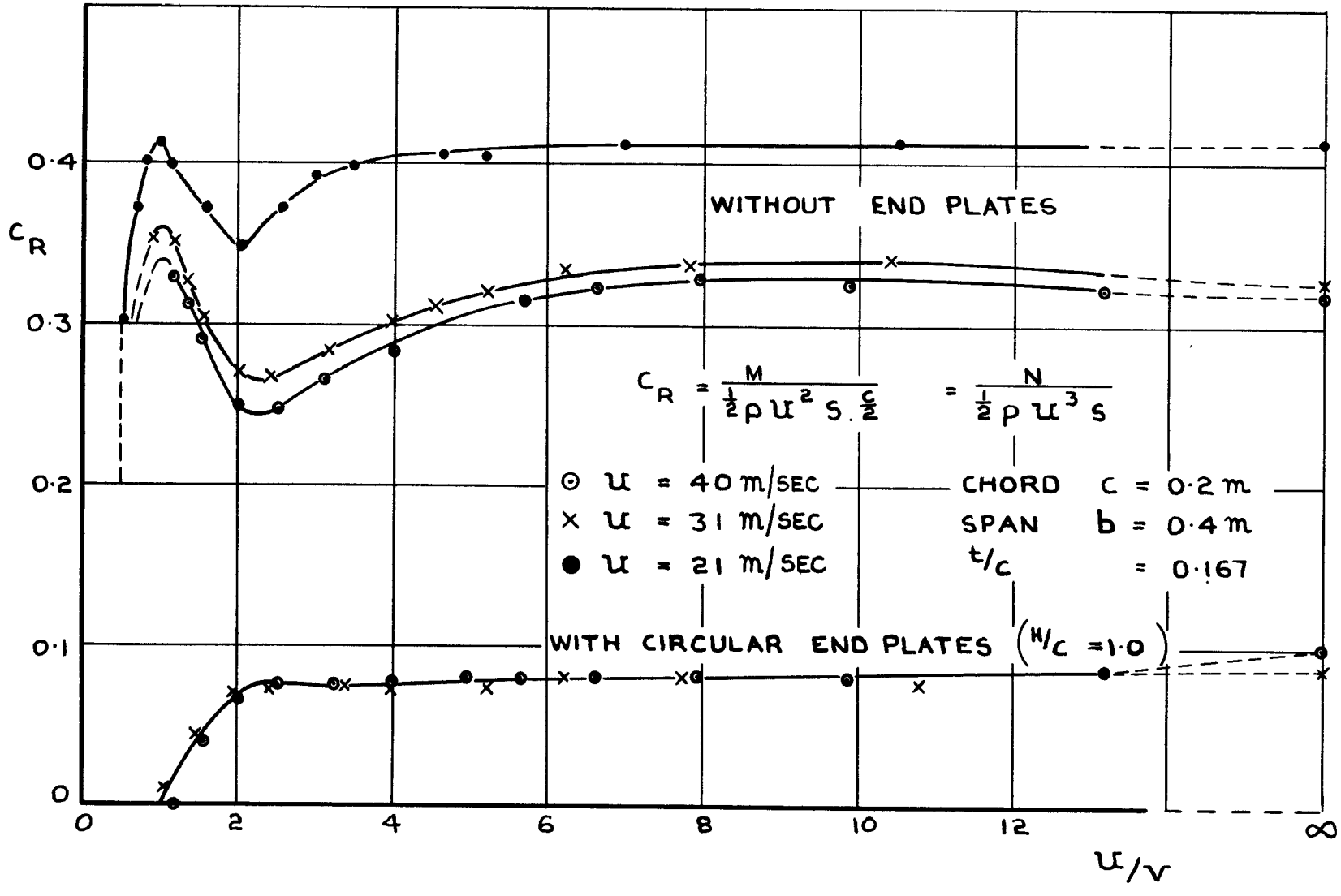

FIG. 4. POWER REQUIRED TO ROTATE A WING OF ASPECT RATIO 2 WITH BICONVEX CIRCULAR-ARC SECTION.

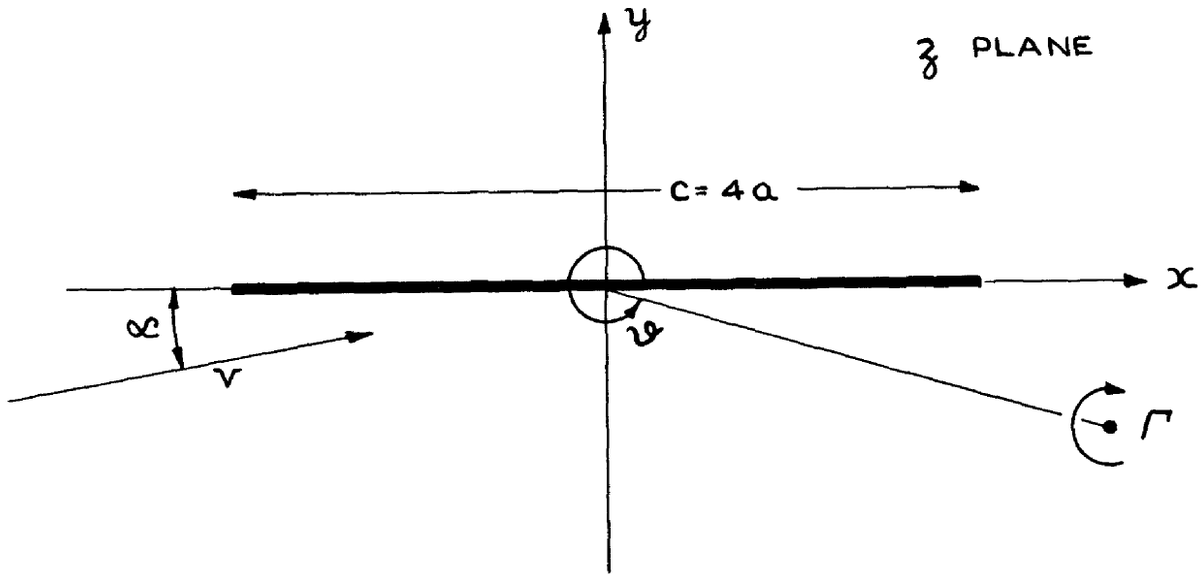

$$z = \zeta + \frac{a^2}{\zeta}$$

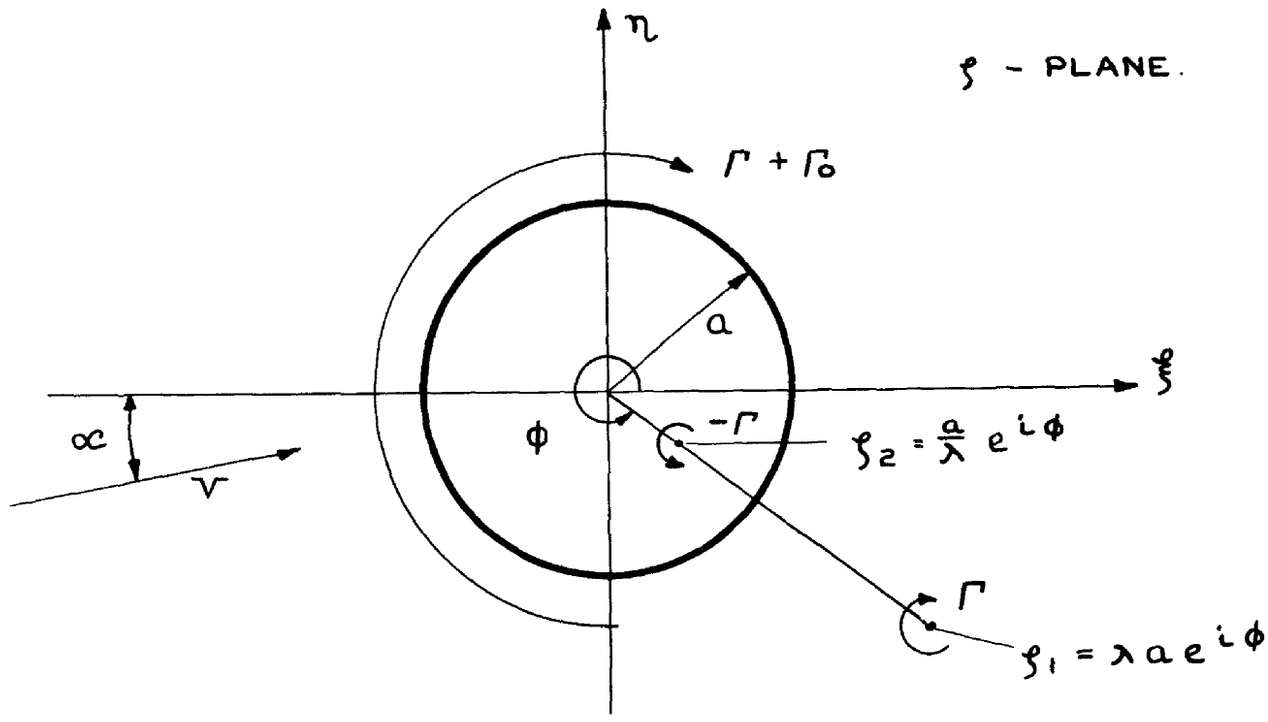

FIG. 5. IDEAL REPRESENTATION OF AN AEROFOIL WITH ROTATING FLAP IN THE z-PLANE AND THE FLOW IN THE CONFORMALLY TRANSFORMED ζ-PLANE.

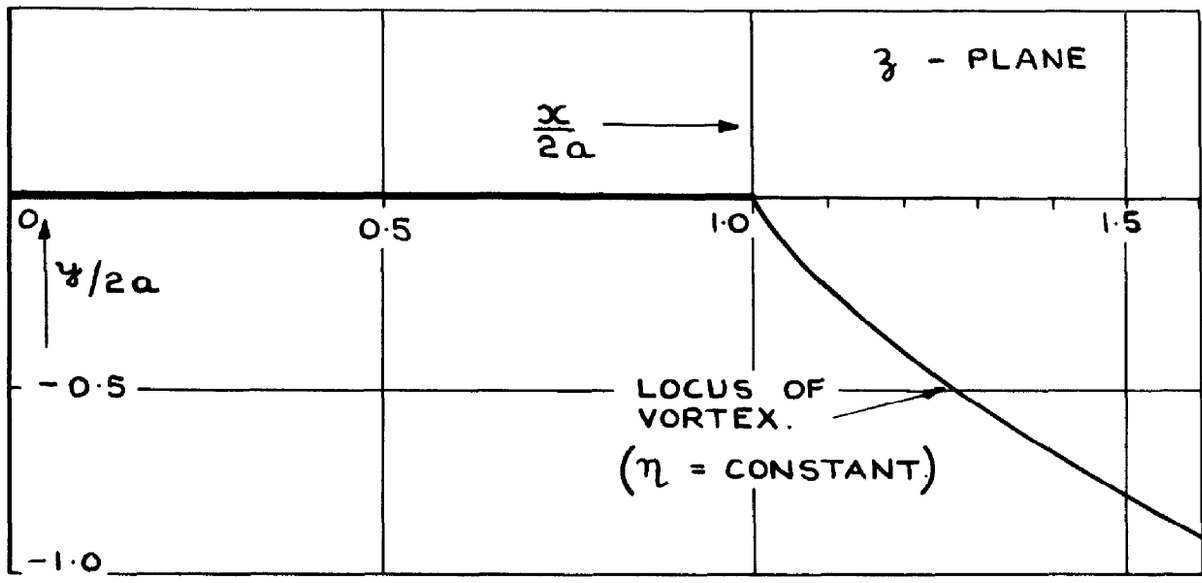

FIG. 6. THEORETICAL BEST POSITION OF A VORTEX REPRESENTING A ROTATING FLAP BEHIND THE TRAILING-EDGE OF AN AEROFOIL.

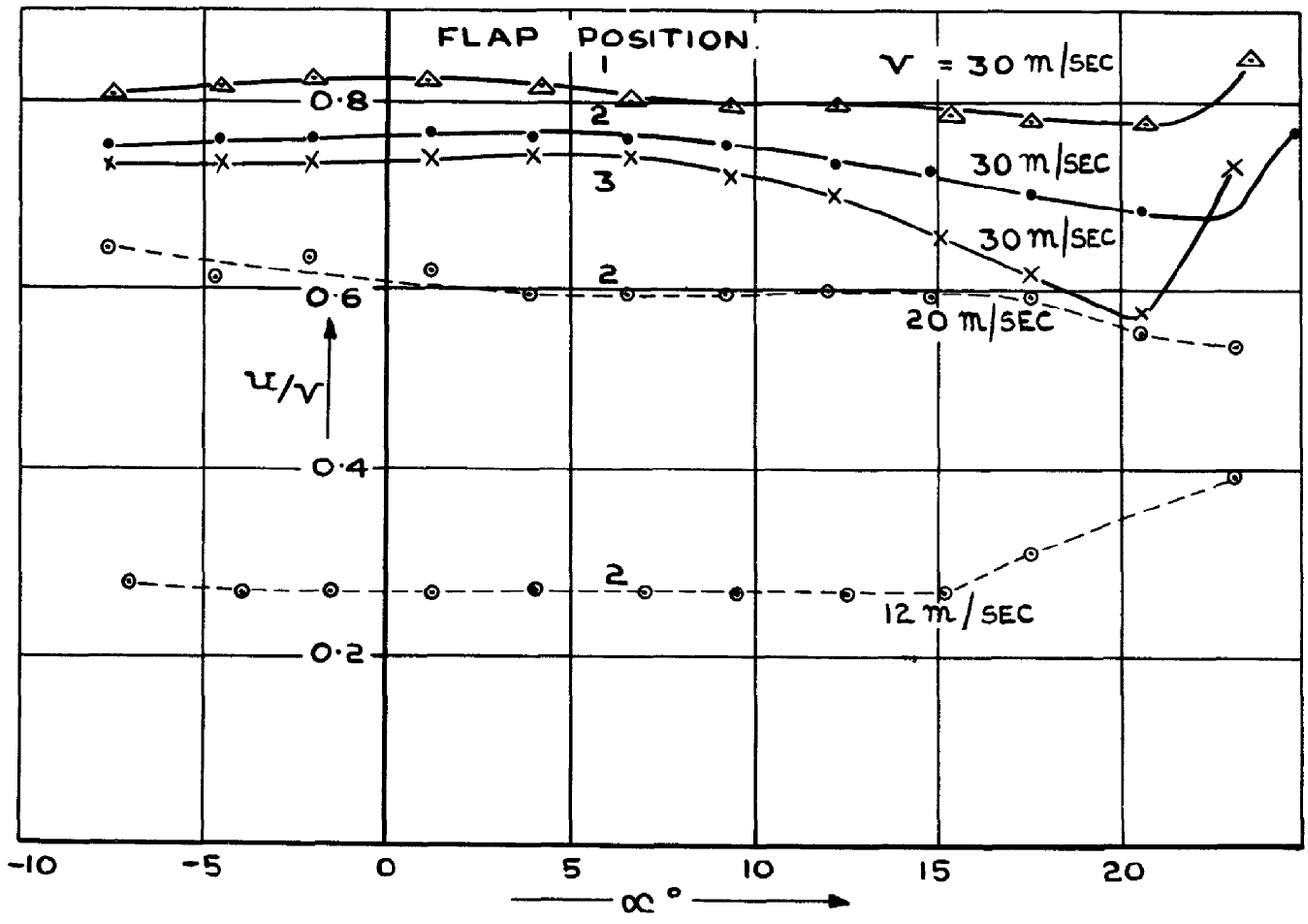

FIG. 7. AUTOROTATION OF FLAP IN DIFFERENT POSITIONS FOR DIFFERENT FREE-STREAM SPEEDS.

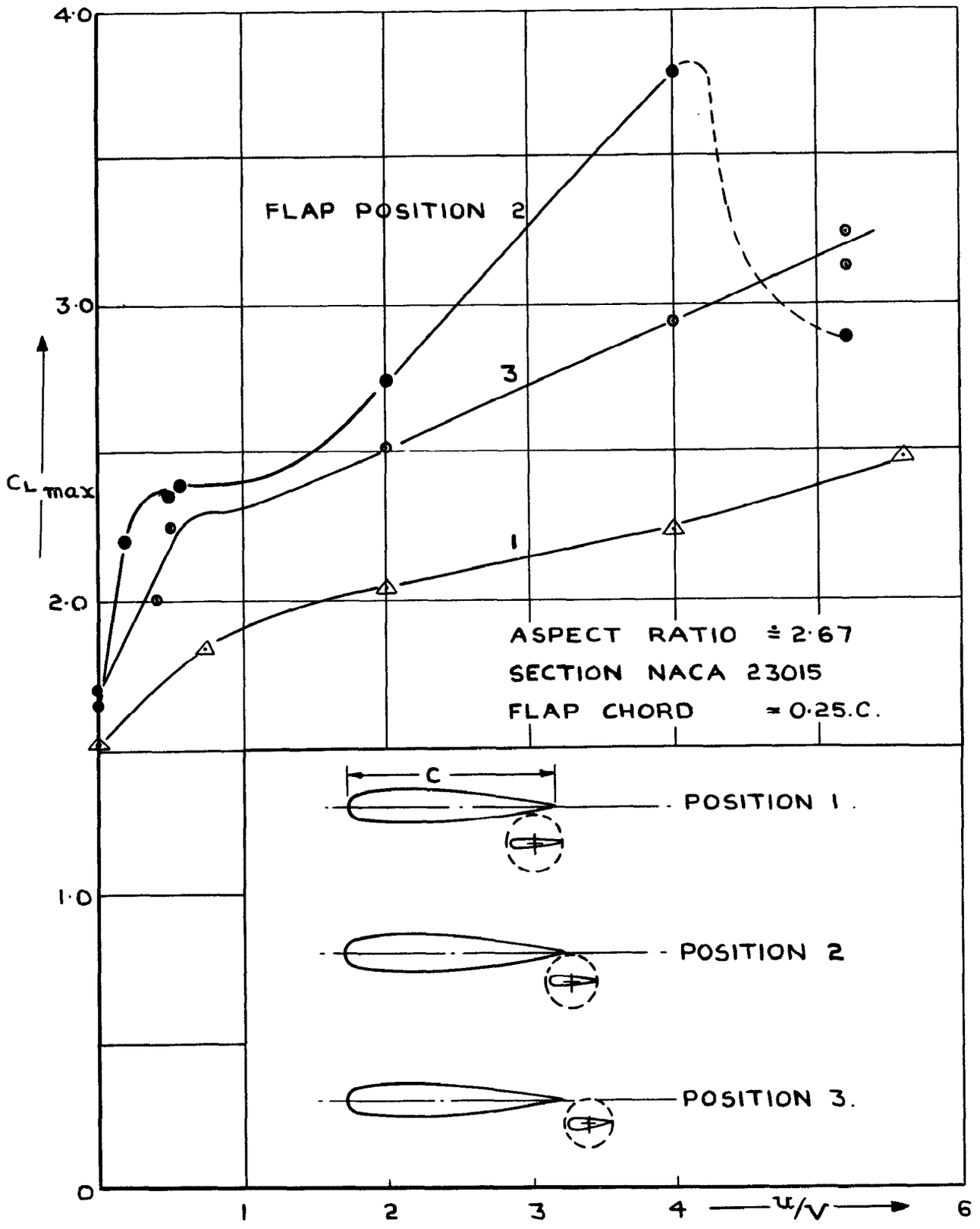

FIG. 8. VALUES OF MAXIMUM LIFT FOR A WING WITH ROTATING FLAP IN DIFFERENT POSITIONS.

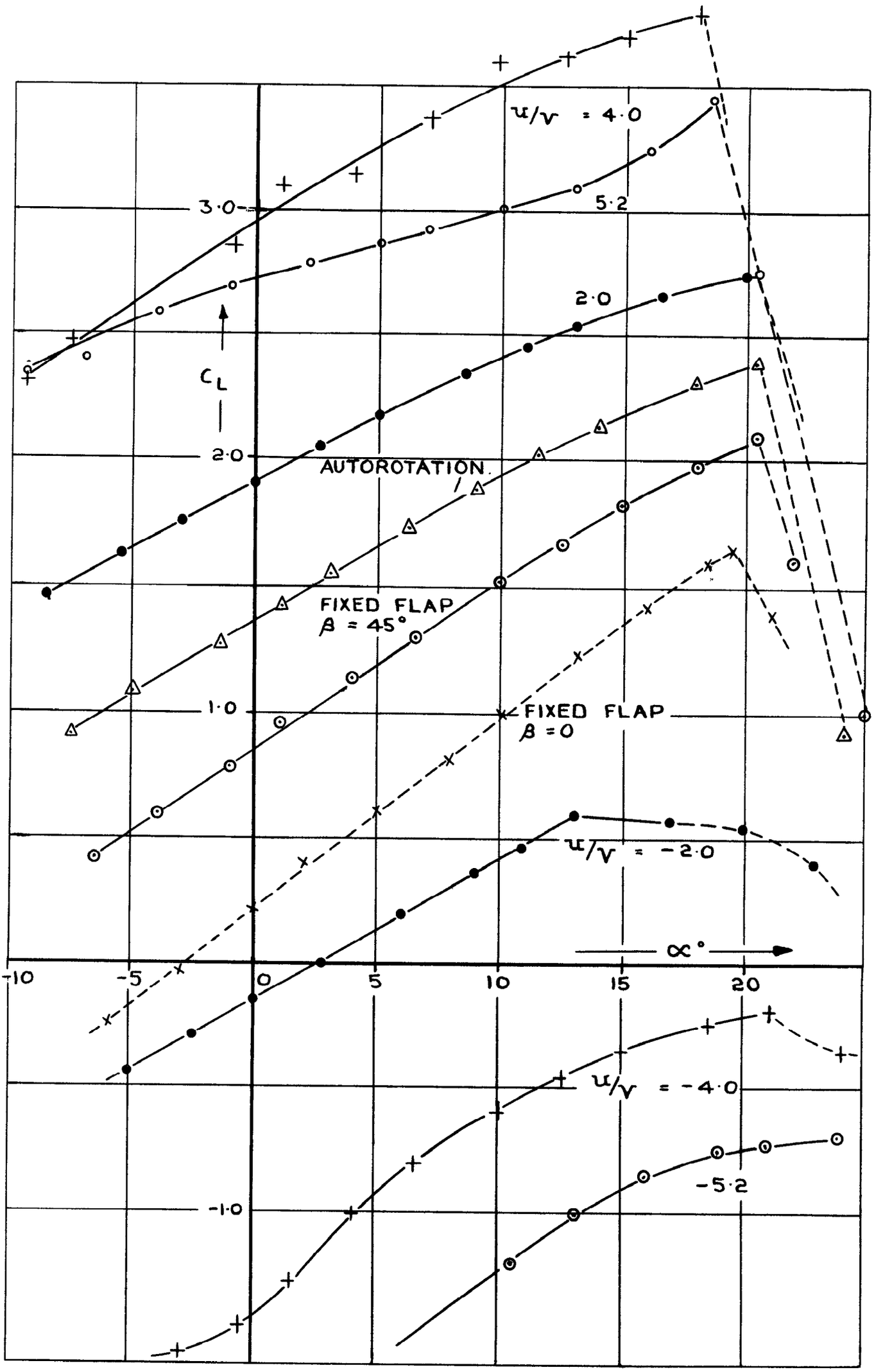

FIG. 9. LIFT CURVES OF WING WITH ROTATING FLAP (POSITION 2.)

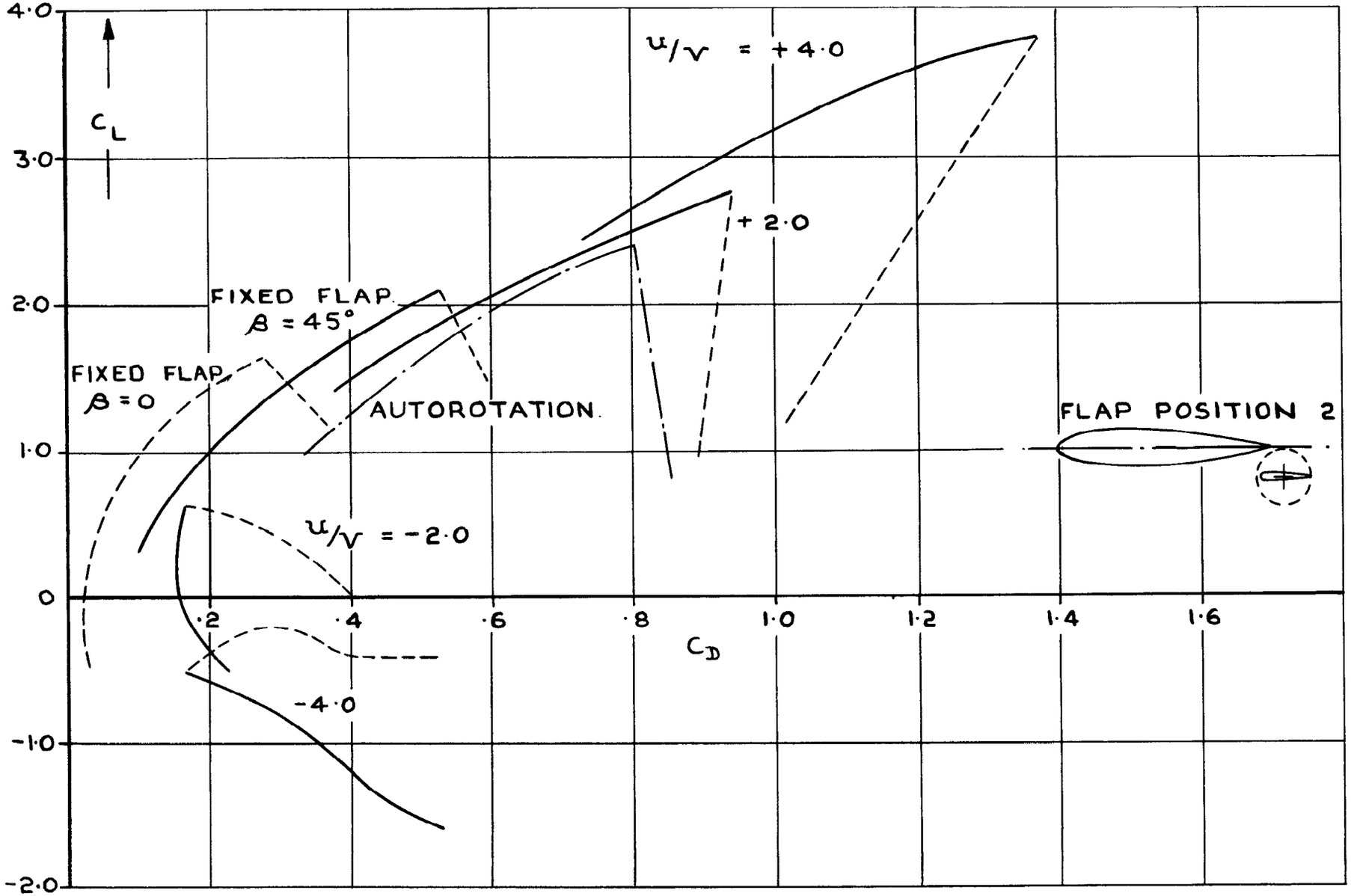

FIG. 10. DRAG POLARS OF A WING WITH ROTATING FLAP (POSITION 2.)

$u/v = -2$

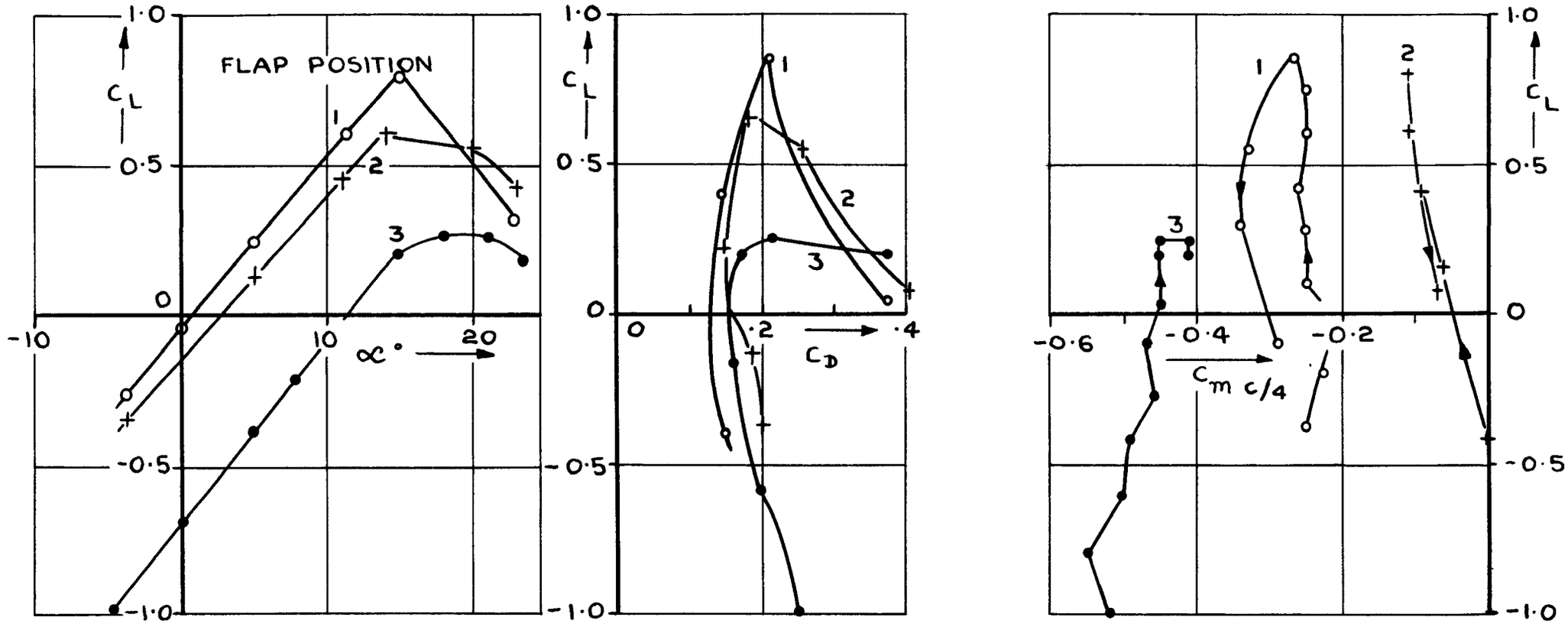

FIG. 11. LIFT, DRAG AND PITCHING MOMENT OF A WING WITH ROTATING FLAP FOR DIFFERENT FLAP POSITIONS AT $u/v = -2$

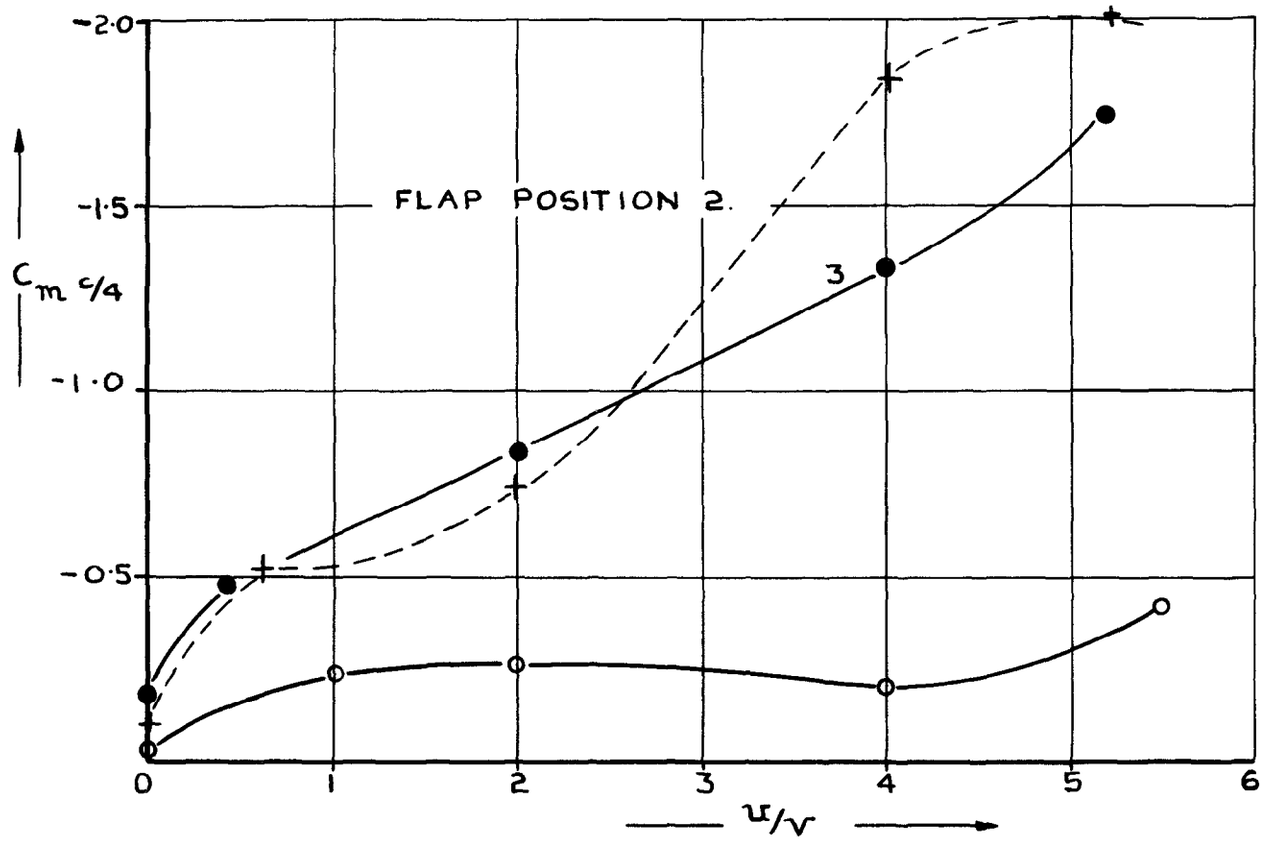

FIG. 12. PITCHING MOMENT AT MAXIMUM LIFT FOR A WING WITH ROTATING FLAP.

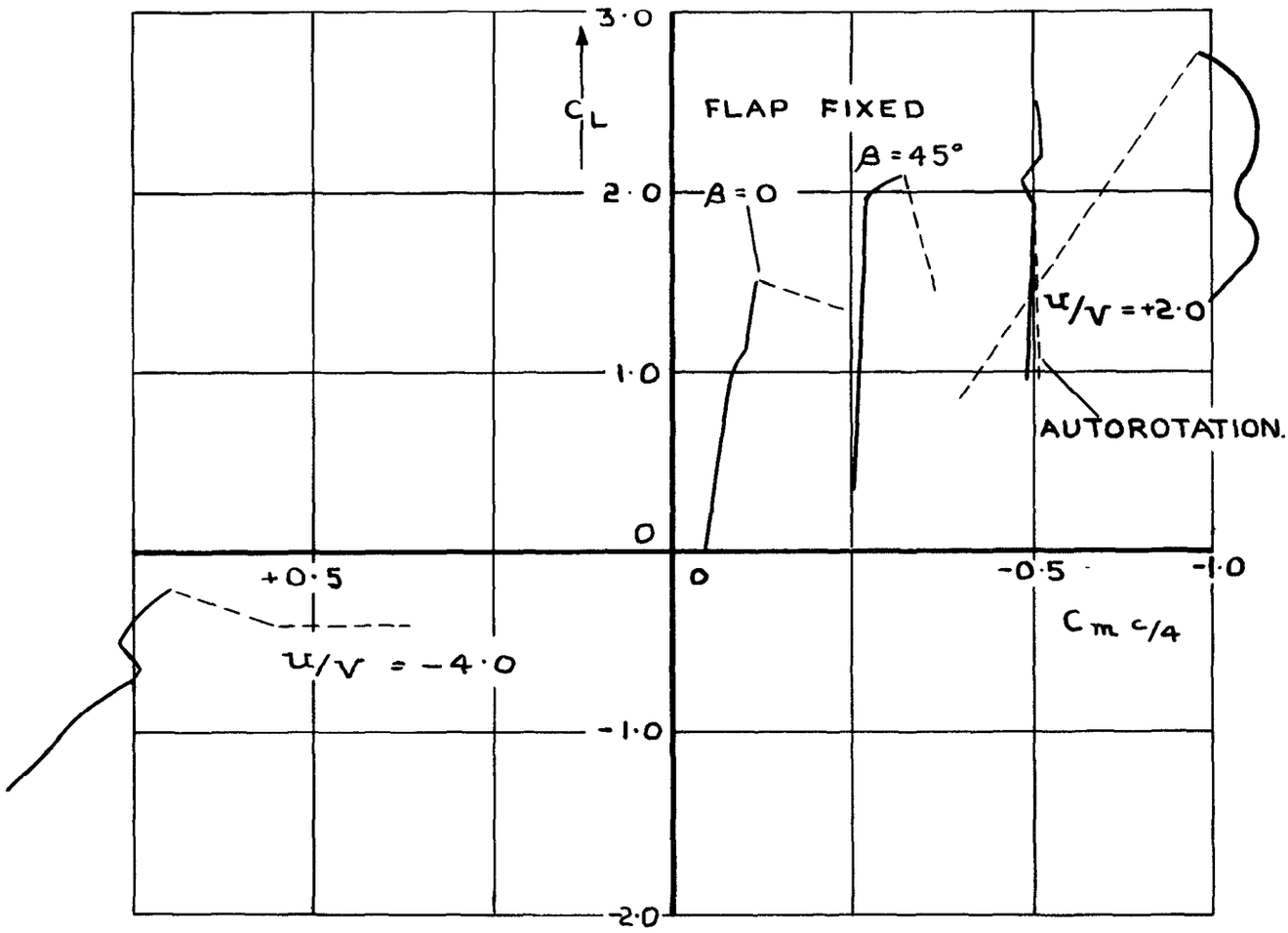

FIG. 13. PITCHING MOMENT OF WING WITH ROTATING FLAP (POSITION 2.)

C.P. No. 480
(19,631)
A.R.C. Technical Report

Published by
HER MAJESTY'S STATIONERY OFFICE

To be purchased from
York House, Kingsway, London w.c.2
423 Oxford Street, London w.1
13A Castle Street, Edinburgh 2
109 St. Mary Street, Cardiff
39 King Street, Manchester 2
Tower Lane, Bristol 1
2 Edmund Street, Birmingham 3
80 Chichester Street, Belfast
or through any bookseller

Printed in England

S.O. Code No. 23-9011-80

C.P. No. 480